Pergamon

Int. J. Heat Mass Transfer. Vol. 41, No. 10, pp. 1157–1166, 1998

Printed in Great Britain
0017–9310/98 $19.00+0.00

PII: S0017–9310(97)00257–3

Numerical modelling of turbulent heat transfer from discrete heat sources in a liquid-cooled channel

G. P. XU, K. W. TOU and C. P. TSO

School of Mechanical and Production Engineering, Nanyang Technological University, Singapore 639798

(*Received* 14 *October* 1996 *and in final form* 13 *August* 1997)

Abstract—Two-dimensional forced convection heat transfer between two plates with flush-mounted discrete heat sources on one plate to simulate electronics cooling is studied numerically using a finite difference method. The two plates form part of a liquid-cooled rectangular channel. The high Reynolds number form of the k–ε turbulence model is used for the computations, which are performed for the liquids water and FC-72 over a range of Reynolds numbers from 10^4 to 1.5×10^5. The numerical procedures and implementation of the k–ε model are validated by comparing the predictions with published experimental data of Mudawar and Maddox [11] and Incropera *et al.* [7] for a single plain heat source as well as with reported multi-chip module data of Incropera *et al.* and Gersey and Mudawar [12]. The effects of the ratio of the channel height to the length of heat source and orientation on the heat transfer characteristics inside the channel are investigated. © 1997 Elsevier Science Ltd.

INTRODUCTION

In the choice of cooling fluid in electronic systems, air is widely used and will always be favored wherever possible because of its economy and its ease of being handled. However, as circuit densities on a single silicon chip continue to increase and as chips are packed in closer proximity on multi-chip modules, power densities continue to rise at both the chip and module levels, dissipating power more than 10 W/cm^2 and beyond, while chip temperature should be maintained below 85°C. As it is becoming increasingly difficult to rely on air cooling to dissipate the heat, liquid cooling is considered, and it may be the only practical method for maintaining reasonable component temperatures in high power chips.

Although numerical investigations of turbulent heat transfer for air cooling of electronic systems were widely reported, including those of Kim and Anand [1], Asako and Faghri [2, 3], Knight and Crawford [4], scant numerical work had been extended to liquid cooling. Heat transfer in laminar flow with one and two heat sources flush-mounted to one wall of a parallel plate channel was considered numerically by Ramadhyani *et al.* [5]. Moffatt *et al.* [6] and Incropera *et al.* [7] numerically predicted turbulent flow in a rectangular channel using a relatively simple model: zero equation turbulent model combined with wall function. Mahaney *et al.* [8] extended the work of Incropera *et al.* to the low Reynolds number regime where mixed convection becomes important.

Experimental studies on forced convection heat transfer from a single plain heat source as well as from a multi-chip module had been carried out for liquid cooling by many investigators. One of the earliest works using silicone oil and R-113 flowing over discrete sources with surface areas ranging from 1 to 200 mm^2 was performed by Baker [9, 10]. Forced convection heat transfer data for a single 12.7 mm square heat source and for a 4×3 array of heat sources were obtained by Incropera *et al.* [7] using water and FC-77 as the working fluid, and it was found that the upstream thermal boundary affected that of downstream. Tests were conducted using a single heat source having the dimensions 12.7×12.7 mm, flush-mounted to one wall of a vertical rectangular channel with 38.1 mm width and 12.7 mm height at atmospheric pressure by Mudawar and Maddox [11], with FC-72 as the coolant. Although the slopes of the correlations obtained by Mudawar and Maddox and by Incropera *et al.* are almost identical, the data of the Mudawar and Maddox was approximately 36 per cent higher than the latter. Experiments were performed by Gersey and Mudawar [12] and FC-72 on a series of nine in-line simulated microelectronic chips in a flow channel to ascertain the effect of orientation angle on the forced convection. The simulated chips, measuring 10×10 mm, were flush-mounted to one wall of a 20×5 mm flow channel. However, they found that the upstream thermal boundary had no effect on that of downstream, and the data from the nine flush-mounted chips were correlated by a single equation.

The objective of the present work is to study numerically turbulent heat transfer with single and four in-line flush-mounted heat sources for liquid

NOMENCLATURE

C_1, C_2 turbulent modelling constants
C_p specific heat at constant pressure [J/kg K]
C_μ turbulent modelling constant
D_h hydraulic diameter of channel [m]
f friction factor
h heat transfer coefficient [W/m^2 K]
H height of channel [m]
k turbulent kinetic energy [m^2/s^2]
L heat source length in flow direction [m]
L_i distance from inlet to first heat source [m]
Nu_L Nusselt number based on length of heat source, $=hL/\lambda$
P_k production of kinetic energy [Pa]
P_σ parameter defined in equation (13)
Pr Prandtl number
q'' heat flux [W/m^2]
Re_L Reynolds number based on length of heat source, $=v_{in}L/\nu$
s distance between heaters [m]
S source term
T_{in} inlet temperature [°C]
T_w heat source wall temperature [°C]
T_p^+ nondimensional temperature near the wall
u velocity in x-direction [m/s]
v velocity in y-direction [m/s]
v_p^+ nondimensional velocity near the wall
w width of channel [m]
x_p^+ nondimensional distance measured from the wall
Y_L total channel length [m].

Greek symbols
α coefficient in equation (17h)
Γ transport coefficient in general equation
ε turbulence dissipation rate [N/s m^2]
λ thermal conductivity [W/m K]
μ dynamic viscosity [N s/m^2]
ν kinematic viscosity [m^2/s]
ρ density [kg/m^3]
σ_k, σ_ε, σ_t turbulent modelling constants
τ shear stress [N/m^2]
ϕ general variable.

Subscripts
eff effective
f fluid
in inlet
p referring to point P near the wall
t turbulent
x referring to the x-direction
y referring to the y-direction.

coolant (water with $Pr = 5.42$ and FC-72 with $Pr = 9.0$). The standard high-Reynolds number k–ε model and wall function are employed for the computations. The k–ε model is a semi-empirical model that has been proven to provide engineering accuracy in a wide spectrum of turbulent flows, including shear flow and wall-bounded flows. The wall function method is cost-effective as it substantially reduces the computer storage and CPU time. This method is justified since the heat sources in the present study are flush-mounted and there is no rapid change in channel geometry causing strong flow acceleration/retardation or flow separation/reattachment. Consequently, no significant departure from local one-dimensionality in the near-wall region is anticipated. The present results are compared with relevant experimental data. The effects of the orientation of the flow channel and the ratio of channel height to the heat source length on heat transfer are investigated.

MODEL FORMULATION

Description of the problem

The numerical model is formulated based on steady, two-dimensional turbulent heat transfer in a channel formed between two plates as shown in Fig. 1. Two modules are considered; in the first case, a single heat source flush-mounted on the left wall as shown in Fig. 1(a), and in the second case, four in-line heat sources mounted on the left wall as shown in Fig. 1(b).

The right surface is assumed to be adiabatic, while the left is assumed to be heated with constant heat flux q''_w generated from one or more heated elements each of length L and regularly spaced at distance s along the surface. It is assumed that the surface outside the elements is adiabatic. The distance from the channel entrance to the first source, L_i, and the distance from the last source to the channel exit, are each equal to $5L$. For simplicity, the heat sources are assumed to be strips of infinite length in the direction perpendicular to the paper, thus rendering the situation two-dimensional. The working fluid is assumed incompressible, and the fluid properties are constant. A Cartesian coordinate system is set up as shown in Fig. 1.

Governing equations

The given flow field must satisfy the continuity equation

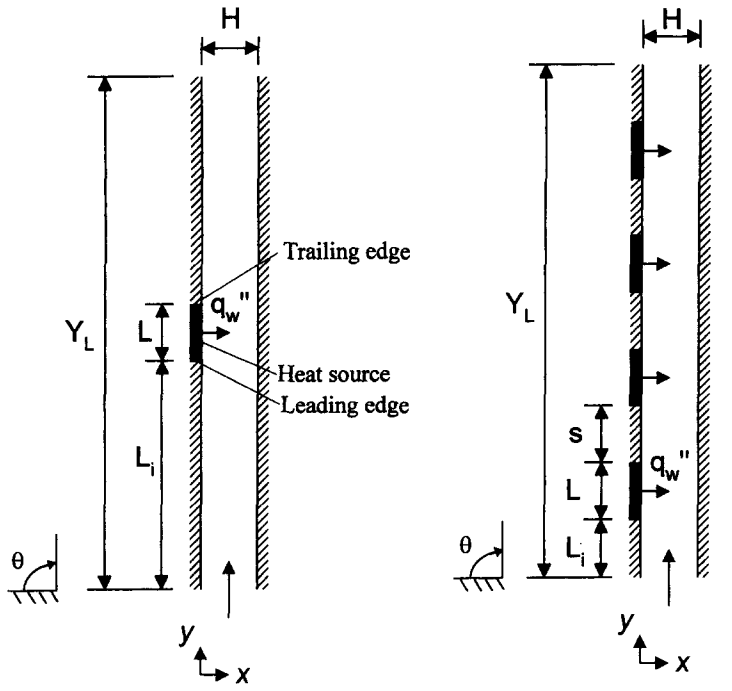

(a) Single heat source (b) Four in-line heat sources

Fig. 1. Physical model for cooling channel in electronic equipment.

$$\frac{\partial(\rho\mu)}{\partial x}+\frac{\partial(\rho v)}{\partial y}=0. \tag{1}$$

Based on the foregoing assumptions, the equation for a general variable transported by convection and diffusion in turbulent flow is given by

$$\frac{\partial(\rho u\phi)}{\partial x}+\frac{\partial(\rho v\phi)}{\partial y}=\frac{\partial}{\partial x}\left(\Gamma\frac{\partial\phi}{\partial x}\right)+\frac{\partial}{\partial y}\left(\Gamma\frac{\partial\phi}{\partial y}\right)+S. \tag{2}$$

In this equation, the general variable ϕ represents u, v, T, k, or ε, where Γ and S represent the appropriate transport coefficient and source term respectively, as shown in Table 1.

In the table,

$$\mu_{\text{eff}}=\mu+\mu_t \tag{3}$$

$$\mu_t=C_\mu\rho k^2/\varepsilon \tag{4}$$

$$P_k=\mu_t\left\{2\left[\left(\frac{\partial u}{\partial x}\right)^2+\left(\frac{\partial v}{\partial y}\right)^2\right]+\left(\frac{\partial u}{\partial y}+\frac{\partial v}{\partial x}\right)^2\right\}. \tag{5}$$

For horizontal flow, $\theta=0°$; for vertical upflow, $\theta=90°$.

Wall function

For completion of the problem formulation, the wall function method is employed near the channel wall. Since a finite difference method is used, the boundary condition should be specified in terms of wall fluxes between the wall and the adjacent grid point (denoted by P) as shown in Fig. 2. The region close to a solid wall can be divided into two sublayers, (a) a laminar or viscous sublayer where viscous effects are dominant and (b) a turbulent sublayer. The wall velocity can be obtained from Launder and Spalding [14] as:

Table 1. General variables and corresponding diffusion coefficients and sources

ϕ	Γ	S
u	$\mu+\mu_t$	$-\partial p/\partial x+\partial[\mu_{\text{eff}}(\partial u/\partial x)]/\partial x+\partial[\mu_{\text{eff}}(\partial v/\partial x)]/\partial y-\rho g\cos\theta$
v	$\mu+\mu_t$	$-\partial p/\partial y+\partial[\mu_{\text{eff}}(\partial u/\partial y)]/\partial x+\partial[\mu_{\text{eff}}(\partial v/\partial y)]/\partial y-\rho g\sin\theta$
T	$\mu/Pr+\mu_t/\sigma_T$	0
k	$\mu+\mu_t/\sigma_k$	$P_k-\rho\varepsilon$
ε	$\mu+\mu_t/\sigma_\varepsilon$	$(C_1P_k\varepsilon-C_2\rho\varepsilon^2)/k$

$C_1=1.44$, $C_2=1.99$, $C_\mu=0.09$, $\sigma_k=1.0$, $\sigma_\varepsilon=1.3$, $\sigma_t=0.9$ [13].

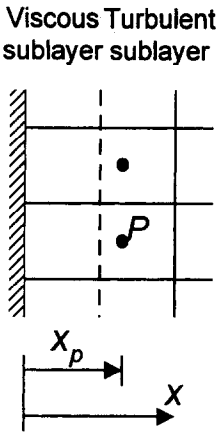

Fig. 2. Location of points adjacent to wall.

$$v_p^+ = 2.5 \ln x_p^+ + 5.5, \quad \text{for } x_p^+ > 11.5 \tag{6}$$

$$v_p^+ = x_p^+, \quad \text{for } x_p^+ \leqslant 11.5 \tag{7}$$

where

$$x_p^+ = \frac{x_p (C_\mu^{1/4} k_p^{1/2})}{\nu} \tag{8}$$

$$v_p^+ = \frac{v_p (C_\mu^{1/4} k_p^{1/2})}{\tau_w/\rho} \tag{9}$$

$$\tau_w = \mu_t \frac{v_p - v_w}{x_p}. \tag{10}$$

The wall turbulent viscosity at point P can be calculated from

$$\mu_t = \frac{x_p^+ \mu}{v_p^+}. \tag{11}$$

The wall temperature can be obtained from [1] as

$$T_p^+ = \frac{(T_w - T_p)\rho C_p C_\mu^{1/4} k_p^{1/2}}{q_w''} = \sigma_t [2.5 \ln(9 x_p^+) + P_\sigma] \tag{12}$$

where

$$p_\sigma = 9 \left(\frac{Pr}{\sigma_t} - 1 \right) \left(\frac{Pr}{\sigma_t} \right)^{-1/4}. \tag{13}$$

The relation between the heat flux and temperature at the wall surface is given by Fourier's law as

$$q_w'' = \lambda_t \frac{T_w - T_p}{x_p} \tag{14}$$

where λ_t is the thermal conductivity in the fluid between the wall and the position P. On rearranging,

$$\lambda_t = \frac{x_p^+ \mu c_p}{\sigma_t [2.5 \ln(9 x_p^+) + P_\sigma]}, \quad \text{if } x_p^+ > 11.5. \tag{15}$$

The dissipation rate of kinetic energy is calculated from

$$\varepsilon_p = \frac{C_\mu^{3/4} k_p^{3/2}}{0.4 x_p}. \tag{16}$$

It should be noted that the dissipation rate ε in the ε equation is also employed to prescribe the value near the wall control volume.

Boundary conditions

The boundary conditions are specified as follows

$$\text{At } x = 0, x = H, \quad u = v = 0. \tag{17a}$$

$$\text{At } y = 0, \quad u = 0. \tag{17b}$$

$$\text{At } y = 0, \quad v = v_{\text{in}}. \tag{17c}$$

$$\text{At } y = 0, \quad T = T_{\text{in}}. \tag{17d}$$

At $x = 0, x = H$ (except at the heat sources),

$$\frac{\partial T}{\partial x} = 0. \tag{17e}$$

$$\text{At the heat sources}, \quad q_w'' = -\lambda_f \frac{\partial T}{\partial x}. \tag{17f}$$

$$\text{At the outlet}, \quad y = Y_L, \quad \frac{\partial T}{\partial y} = 0. \tag{17g}$$

Equations (17c) and (17d) prescribe a uniform velocity and a uniform temperature at the channel entrance, and equation (17g) assumes the streamwise energy diffusion flux to be negligible at the outlet.

In view of the situation that the experimental values of k and ε are not known at the inlet, some reasonable assumptions can be made. The inlet kinetic energy of turbulence is estimated according to a certain percentage of the square of the average inlet velocity

$$k_{\text{in}} = \alpha v_{\text{in}}^2 \tag{17h}$$

where v_{in} is the average inlet velocity and α is a percentage between 0.5% and 1.5%, following Patankar *et al.* [15] for fully developed turbulent flow.

The inlet dissipation is calculated according to the equation

$$\varepsilon_{\text{in}} = 0.1 k_{\text{in}}^2 \tag{17i}$$

Prediction results are insensitive to inlet k and ε values [15] since the viscous effects are small compared to the fluid inertia at high Reynolds number. This has been confirmed after a few numerical trials.

The outlet conditions for k and ε are not specified, but are given at the inlet as per equations (17h) and (17i). The problem is then approximated by a one-way space coordinate of parabolic nature under the action of fluid flow and when convection mode of transport dominates the diffusion mode. In this situation, the solution is largely controlled by the upstream condition and very little by the downstream one.

Reynolds number, Nusselt number

For calculation of the Reynolds number, L is selected as the characteristic dimension, that is,

$$Re_L = \frac{v_{in} L}{\nu}. \tag{18}$$

The local Nusselt number is defined as

$$Nu_{L,i} = \frac{hL}{\lambda} = \frac{q''_w L}{(T_{w,i} - T_{in})\lambda} \tag{19}$$

while the average Nusselt number is calculated from

$$Nu_L = \frac{\sum_{i=1}^{m} Nu_{L,i}}{m} \tag{20}$$

where m is the total number of grid points in the heat sources.

NUMERICAL SOLUTION

The numerical procedure Semi-Implicit Method for Pressure-Linked Equation (SIMPLE) is used to solve the basic conservation equations. The finite volume technique has been described in detail by Patanker [16]. This algorithm provides a remarkably successful implicit method for simulating incompressible flow including those involved in the cooling of electronic equipment [1–3, 17]. The set of discretization equations for each variable is solved by the line by line procedure, which is the combination of the Tri-Diagonal Matrix Algorithm (TDMA) and the Gauss–Seidal iteration technique. The SIMPLE algorithm solves the pressure equation to obtain the pressure field and solves the pressure-correction equation to correct the velocities.

The convergence criterion used in this computation is that the value of the mass flux residuals (mass flow) R_{sum} in each control volume takes a value less than 10^{-9}, and relative values of velocities u and v and temperature cease to vary by more than 10^{-5} between two successive iterations. The under-relaxation factor values for velocity, pressure, turbulence kinetic energy, energy dissipation rate and turbulent viscosity are set to 0.5, 0.8, 0.1–0.4, 0.1–0.4, and 0.5, respectively. A sufficient number of iterations, typically 2000 to 10 000, are performed to obtain a converged solution, with the number of interactions depending on the Reynolds number, the geometry and the working fluid.

Grid-independence

Grid independence is established by examining the wall temperature distribution at the surface of the heat source. A non-uniform mesh with a large concentration of nodes in heat sources is set up. The computational region consists of 50 grid lines in the x-direction and 93 grid lines in the y-direction, the latter including 30 grid lines in the single heat source.

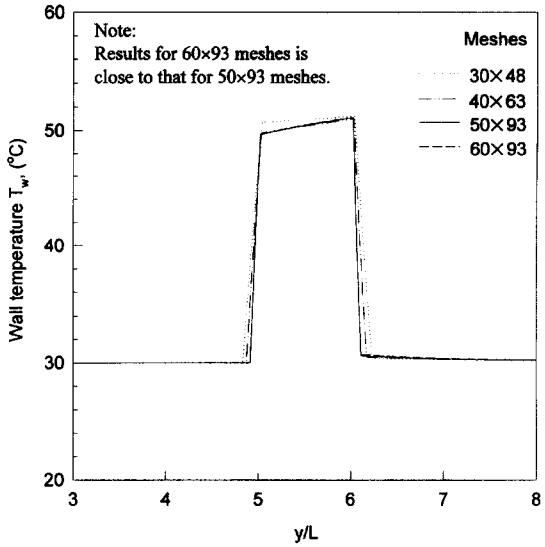

Fig. 3. Effect of grid size on temperature distribution (L = 12.7 mm, H/L = 1, $Re_L = 1.5 \times 10^5$).

For the purpose of the grid independence study, the Re is chosen to be 1.5×10^5. Four different non-uniformly spaced grid sizes are used 30×48 (with 15 grid points in the y-direction of the heat source), 40×63 (with 20 grid points in the y-direction of the heat source), 50×93 and 60×93 (with 30 grid points in the y-direction of the heat source). The wall temperature distribution for the various grid sizes and the Nusselt numbers are shown in Fig. 3 and Table 2, respectively. Grid independence is declared when maximum changes in temperature distribution, Nusselt number and friction factor are less than 3%. The results from the last three grids are acceptable.

RESULTS AND DISCUSSIONS

Single plain heat source

Figure 4 shows the comparison of the numerically predicted with the experimentally determined Nusselt number obtained by Mudawar and Maddox [11] for the single plain heat sources using FC-72 as the working fluid. The numerical results agree well with the experimental data, with differences of about 10%.

Figure 5 shows the wall temperature distributions at Reynolds number 7×10^4 and 1.5×10^5, respec-

Table 2. Effect of grid size on Nusselt number and friction factor ($Re_L = 1.5 \times 10^5$, Pr = 9.0, FC-72)

Grid	Nu_L	f
20×48	980.9	0.0117
30×48	1113.0	0.0132
40×63	1142.0	0.0136
50×93	1141.0	0.0136
60×93	1139.0	0.0135

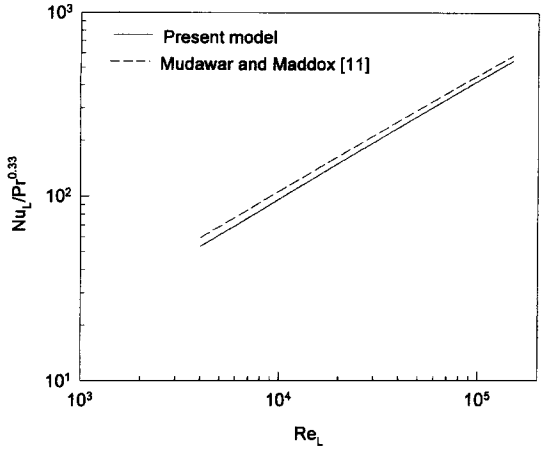

Fig. 4. Comparison of present model with the experimental data of Mudawar and Maddox [11] ($H/L = 1$, $L = 12.7$ mm).

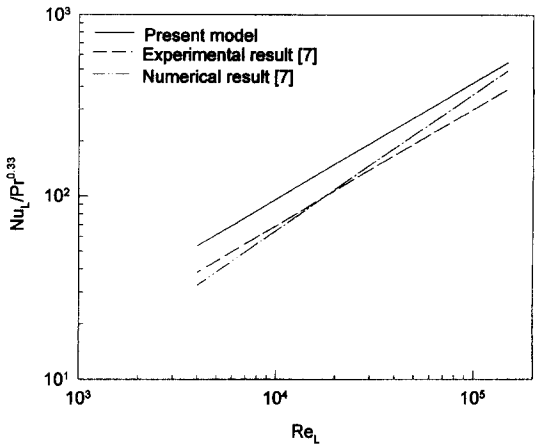

Fig. 6. Comparison of present model with the experimental dat and numerical results of Incropera *et al.* [7] ($H = 11.9$ mm, $L = 12.7$ mm).

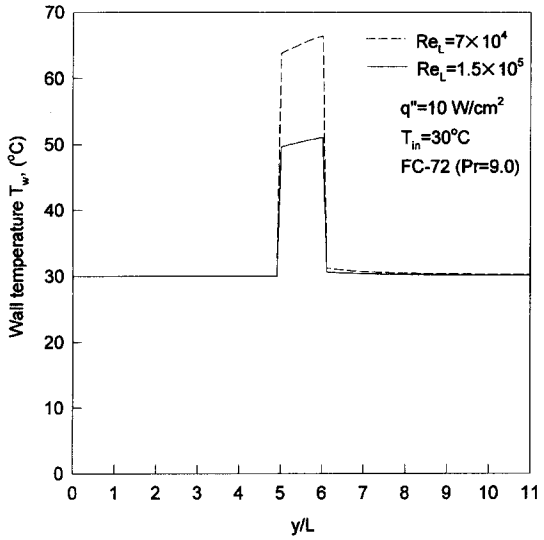

Fig. 5. Distributions of wall temperatures.

tively. The wall temperatures are sharply peaked at the leading edge of the heat source and increase with increasing distance to the trailing edge. The trend of the result is similar to the results obtained by Ramadhyani *et al.* [5] for laminar flow, and by Moffatt *et al.* [9] for turbulent flow. However, the Nusselt number predicted by the present model is about 30% higher than that by the zero equation turbulent model used by Moffatt *et al.* [6]. Compared to the experimental results and numerical results reported by Incropera *et al.* [7] for the single plain heat source using water and FC-77 as the working fluid, it is found that the result predicted by the present model is also about 30% higher than their results as shown in Fig. 6.

Flow and thermal field analysis

The representative velocity vectors are presented in Fig. 7, showing that the velocity is quite uniform in the channel. This may be due to the wall function method being used in the present formulation so that the velocity near the wall cannot be detailed by the numerical method. Another reason may be that there is no obstacle in the flow channel, as the simulated electronic chip is flush-mounted on the wall.

The velocity profiles in the y-direction at three channel locations ($y/L = 4.92$, 5.55 and 6.12) are shown

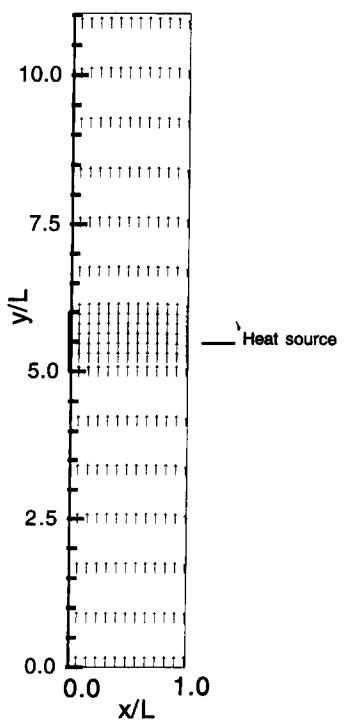

Fig. 7. Predicted velocity vector plot ($Re_L = 7 \times 10^4$, FC-72).

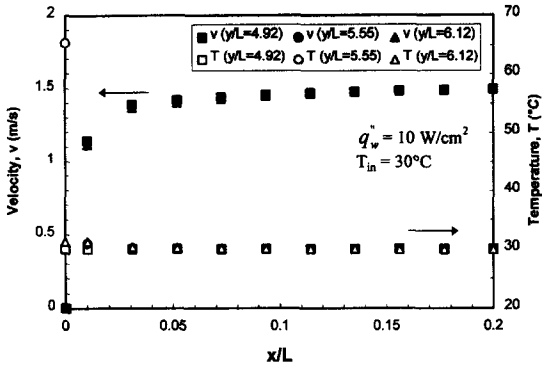

Fig. 8. Velocity profiles and temperature profiles at the middle of and near the heat source ($Re_L = 7 \times 10^4$, FC-72).

in Fig. 8. It is found that the velocity profiles for the turbulent flow is flat with velocity increasing sharply at the first point near the wall; the velocity near the wall is defined by the wall function.

The temperature distributions in the flow channel near the wall have also be studied and given in Fig. 8 at the same locations. The results are similar to those of velocity, but the temperature distributions are more uniform than those of velocity. This temperature profile suggests that there is practically no heat transfer in the fluid across the channel as the heat transfer process has been dominated and completed near the wall. The direct liquid cooling of electronic chips is different from the air cooling in that the temperature difference of the liquid between the entrance and the exit of the channel is small, less than 0.5°C as calculated from the energy balance equation. However, because the heat capacity (ρC_p) of liquid is generally much higher than that of air, the heat flux dissipated by the electronic chips in liquid cooling is higher. The temperature in the first point near the wall is very close to the inlet temperature. The temperature distributions between the first point and the wall also have been specified by the wall function. The temperature distribution before the heat source ($y/L = 4.92$) is a little lower than that after the heat source ($y/L = 6.12$), showing that the effect of the upstream thermal boundary layer on the downstream is weak. Similar experimental results were reported by Gersey and Mudawar [12].

Effect of channel height on heat transfer performance

The effect of the geometric parameter, expressed by the ratio of channel height to the heat source length H/L, on the average Nusselt number at $Re_L = 7 \times 10^4$ is shown in Table 3. It is found that the ratio H/L has little effect on the Nusselt number in the range of 1 to 0.125. The average Nusselt number decreases slightly with increases in the ratio. For example, the difference in average Nusselt number between the ratio $H/L = 1$ and $H/L = 0.5$ is only 5%. Similar results were obtained by Gersey and Mudawar in experimental multi-chip cooling using FC-72 as the working fluid.

Table 3. The effect of H/L on average Nusselt number ($Re_L = 7 \times 10^4$, FC-72)

H/L	Nu_L
1.0	661.2
0.5	691.7
0.25	781.3
0.125	882.5

They found that the experimental data of $H/L = 0.5$ and $H/L = 0.2$ can be correlated by the same correlation; the channel height has little effect on the average Nusselt number. A weak dependence on H/L was also founded by Incropera *et al.* by using their numerical computation. The effect of ratio of channel height to the length of heat source H/L on the wall temperature distribution is shown in Fig. 9.

However, for the air cooling of protruded discrete heat sources, the effects are noticeable. Kim and Anand [1] numerically showed that the average Nusselt number is proportional to $(H/L)^{-0.814}$ in turbulent flow. McEntire and Webb [19] experimentally showed that the average Nusselt number is proportional to $(H/L)^{-0.40}$ in the range of $10^3 < Re_L < 10^4$. Olivos and Majumdar [20] numerically showed that the average Nusselt number decreases with increases in the ratio of channel height to length of heat source H/L in laminar flow. It is anticipated that their temperature profile is not as uniform as in the present case in a liquid-cooled channel.

Effect of orientation on the single-phase forced convection heat transfer

The effect of orientation on the forced convection heat transfer is studied as shown in Table 4. It is found

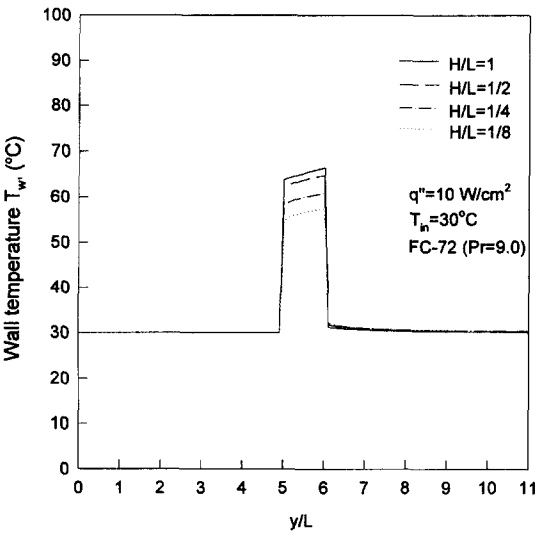

Fig. 9. Effect of H/L on the distribution of wall temperature ($Re_L = 7 \times 10^4$).

Table 4. Effect of orientation on the average Nusselt number (FC-72)

	$Re_L = 2\times10^4$	$Re_L = 7\times10^4$	$Re_L = 1.5\times10^5$
Horizontal flow ($\theta = 0°$)	$Nu_L = 336.0$	$Nu_L = 661.2$	$Nu_L = 1141$
Vertical upflow ($\theta = 90°$)	$Nu_L = 336.2$	$Nu_L = 661.0$	$Nu_L = 1141$

that orientation has no or little effect on the forced convection. The result is consistent with the conclusion that body force terms in the governing equations can be neglected for forced convection [21]. The result can also be supported from the order of magnitude analysis on dimensionless groups in the governing equations. The effect of orientation had also been investigated experimentally for nine in-line discrete heat sources by Gersey and Mudawar [3]. Similar results were obtained from their study; whose data for different angles of orientation were correlated well by a single correlation, and there were no dimensional or dimensionless item reflecting the angle and body force in the correlation. From both numerical and experimental results, it is concluded that orientation has little effect on forced convection heat transfer in direct liquid cooling. But the effects of orientation on heat transfer must be considered in free convection and phase change circumstances.

Four in-line heat sources

Figure 10 shows the comparison between the numerically predicted results for the four in-line heat sources (as in Fig. 1(b)) and the experimentally determined Nusselt number obtained by Incropera *et al.* using water as the working fluid. Although all the chips have similar heat transfer coefficients, it is found that the Nusselt number for the first chip is slightly higher than the values of other chips as predicted by present model. However, not only the experimental data of Incropera *et al.* are about 30% lower than the values predicted by present model, but the effect of the number of rows of heat sources on heat transfer coefficient is also inconsistent with the present model. They reported that, for an array of the heat sources consisting of four rows of three sources per row, upstream thermal boundary layer development causes the average Nusselt number to decrease with increasing row number, until a fully-developed condition is reached at approximately the fourth row. Values for the first row were considerably larger than those for the last three rows, with the percentage difference between the rows decreasing with increasing Reynolds number. But the present study finds that the number of chips have little effect on the thermal boundary layer.

Compared to the experimental data obtained by Gersey and Mudawar with FC-72 on a series of nine in-line simulated chips in a flow channel, the numerical data agree well with their results as shown in Fig. 11. Because Gersey and Mudawar found that the nine in-line simulated chips had same heat transfer coefficients, all the data from the nine flush-mounted chips were correlated by a single correlation.

Figure 12 shows the wall temperature distributions of four in-line heat sources for FC-72 at Reynolds

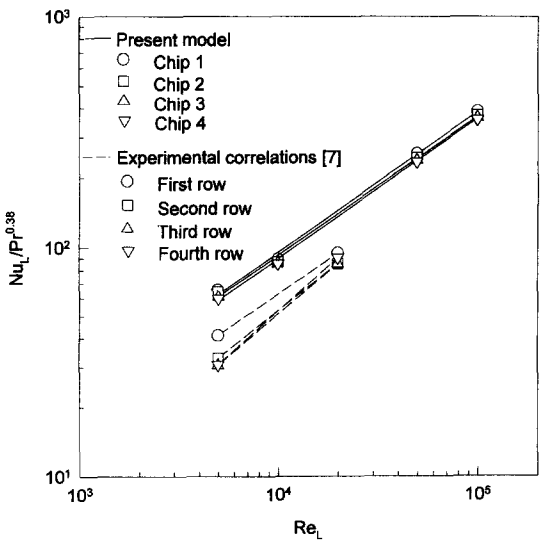

Fig. 10. Comparison of predictions and the experimental data of Incropera *et al.* [7] for four rows of heat sources.

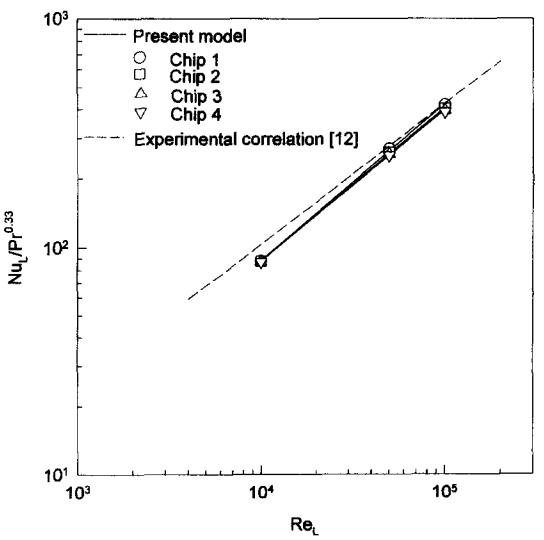

Fig. 11. Comparison of prediction and the experimental data of Gersey and Mudawar [12] for multi-chip module.

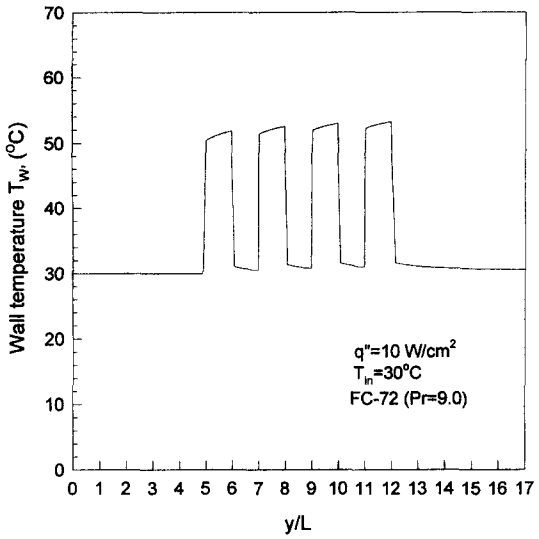

Fig. 12. The wall temperature distributions for four in-line heat sources with FC-72 ($Re_L = 1 \times 10^5$).

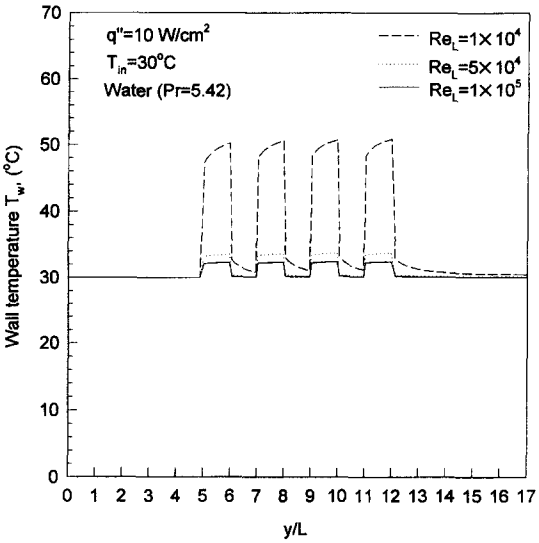

Fig. 13. The wall temperature distributions for four in-line heat sources with water.

number 1×10^5. There is little change in temperature distribution among chips. The wall temperature distributions of water are shown in Fig. 13 which also indicates that the number of chips have little effect on the wall temperature.

CONCLUSIONS

Direct liquid cooling of simulated chips in a rectangular channel has been studied numerically by solving the two-dimensional governing equations using the k–ε model for turbulent closure. The key findings are as follows:

1. The solution technique is validated by comparing the experimental data for a single plain heat source in a rectangular channel [11].
2. The wall temperatures are sharply peaked at the leading edge of the heat source and increase with increasing distance to the trailing edge.
3. The numerical studies suggest that the heat transfer process is dominated near the wall of the heat sources and as a result a narrow channel with small H/L can be used for liquid cooling.
4. The average Nusselt number predicted by present model is about 30% higher than the experimental results and numerical results reported by Incropera *et al.* [7].
5. The average Nusselt number decreases slightly with increases in the ratio of channel height to the length of heat source. It is concluded that the thermal conditions are more representative of external flow.
6. The orientation of flow channel has little effect on forced convective heat transfer in liquid cooling.
7. For four plain heat sources, all heat sources have similar single-phase heat transfer coefficients.
8. Compared to the experimental data obtained by Gersey and Mudawar [12] for multi-chip module, the numerical data agree well with their data. However, present results are inconsistent with the data of Incropera *et al.* [7].

REFERENCES

1. Kim, S. H. and Anand, N. K., Turbulent heat transfer between a series of parallel plates with surface-mounted discrete heat sources. *ASME Journal of Heat Transfer*, 1994, **116**, 577–587.
2. Asko, Y. and Faghri, M., Three dimensional heat transfer analysis of arrays of heated square blocks. ASME HTD-Vol. 171, 1991, pp. 135–141.
3. Asko, Y. and Faghri, M., Prediction of turbulent heat transfer in the entrance of an array of heated blocks using low-Reynolds-number k–ε model. *Numer. Heat Transfer*, 1995, Part A, **28**, 263–277.
4. Knight, R. W. and Crawford, M. E., Numerical prediction of turbulent flow and heat transfer in channels with periodically varying cross sectional area. *Proceedings of the* 1988 *National Heat Transfer Conference*, ASME, Vol. 1, 1988, pp. 669–676.
5. Ramadhyani, S., Moffatt, D. F. and Incropera, F. P., Conjugate heat transfer from small isothermal heat sources embedded in a large substrate. *International Journal of Heat and Mass Transfer*, 1985, **28**, 1945–1952.
6. Moffatt, D. F., Ramadhyani, S. and Incropera, F. P., Conjugate heat transfer from wall embedded sources in turbulent channel flow. In *Heat Transfer in Electronic Equipment*, ed. A. Bar-Cohen, ASME HTD-Vol. 57, 1986, pp. 177–182.
7. Incropera, F. P., Kerby, J. S., Moffatt, D. F. and Ramadhyani, S., Convection heat transfer from discrete heat sources in a rectangular channel. *International Journal of Heat and Mass Transfer*, 1986, **29**, 1051–1058.
8. Mahaney, H. V., Incropera, F. P. and Ramadhyani, S., Comparison of predicted and measured mixed convection heat transfer from an array of discrete sources in a horizontal rectangular channel. *International Journal of Heat and Mass Transfer*, 1990, **33**, 1233–1245.
9. Baker, E., Liquid cooling of microelectronic devices by free and forced convection. *Microelectronics and Reliability*, 1972, **11**, 213–232.
10. Baker, E., Liquid immersion cooling of small electronic

devices. *Microelectronics and Reliability*, 1973, **12**, 163–173.
11. Mudawar, I. and Maddox, D. E., Enhancement of critical heat flux from high power microelectronic heat sources in a flow channel. In *Heat Transfer in Electronics*, ed. R. K. Shah, ASME HTD-Vol. 111, 1989, pp. 51–58.
12. Gersey, C. O. and Mudawar, I., Effects of orientation on critical heat flux from chip arrays during flow boiling. In *Advances in Electronic Packaging*, Vol. 1, ed. T. C. William and A. Hiroyuki, ASME, New York, 1992, pp. 123–134.
13. Markatos, N. C., The mathematical modelling of turbulence flows. *Appl. Math. Modelling*, 1986, **10**, 190–220.
14. Launder, B. E. and Spalding, D. B., The numerical computation of turbulent flows. *Comp. Methods Appl. Mech. Eng.*, 1974, **3**, 269–289.
15. Patankar, S. V., Sparrow, E. M. and Ivanovic, M., Thermal interaction among the confining walls of a turbulent recirculating flow. *International Journal of Heat and Mass Transfer*, 1978, **24**, 269–274.
16. Patankar, S. V., *Numerical Heat Transfer and Fluid Flow*. Hemisphere Publishing Company, New York, 1980.
17. Kim, S. H. and Anand, N. K., Laminar developing flow and heat transfer between a series of parallel plates with surface-mounted discrete heat sources. *International Journal of Heat and Mass Transfer*, 1994, **37**, 2231–2244.
18. Gersey, C. O. and Mudawar, I., Nucleate boiling and critical heat flux from protruded chip arrays during flow boiling. *ASME Journal of Electronic Packaging*, 1993, **115**, 78–88.
19. McEntire, A. B. and Webb, B. W., Local forced convective heat transfer from protruding and flush-mounted two-dimensional discrete heat sources. *International Journal of Heat and Mass Transfer*, 1990, **33**, 1233–1245.
20. Olivos, T. and Majumdar, P., A computational model for forced convection cooling in electronic components. *Journal of Electronics Manufacturing*, 1995, **5**, 183–192.
21. Tao, W. Q., *Numerical Heat Transfer*. Xi'an Jiaotong University Press, PRC (in Chinese), 1988.